THERMAL TRANSPORT TO DROPLETS IMPINGING ON HORIZONTAL SUPERHYDROPHOBIC SURFACES

Jonathan C. Burnett
Department of Mechanical Engineering
Brigham Young University
Provo, Utah 84602

Dan Maynes*
Julie Crockett
Department of Mechanical Engineering
Brigham Young University
Provo, Utah, 84602

ABSTRACT

An analytical model is developed to quantify the heat transfer to droplets impinging on heated superhydrophobic surfaces. Integral analysis is used to incorporate the apparent temperature jump at the superhydrophobic surface as a boundary condition. This model is combined with a fluid model which incorporates velocity slip to calculate the cooling effectiveness, a metric outlined in contemporary work. The effect of varying velocity slip and temperature jump is analyzed for different impact Weber numbers and surface temperature ranging from 60 to 100 °C. Heat transfer to the drop on superhydrophobic surfaces is decreased when compared to conventional surfaces.

NOMENCLATURE

C_p Specific Heat
D Droplet Diameter
D_0 Initial Droplet Diameter
H Droplet Height
k Heat Conductivity
m Mass
Oh Ohnesorge Number
R Droplet Radius
t Time Since Droplet Impact
T Temperature
T_c Contact Temperature
T_{dr} Initial Droplet Temperature
q''_w Wall Heat Flux
V_0 Initial Droplet Velocity
We Weber number, $We = \rho V_0^2 D/\sigma$
α Thermal Diffusivity
δ_T Thermal Boundary Layer Thickness
ε Cooling Effectiveness
γ Thermal Effusivity
λ Slip Length
λ_T Thermal Slip Length
ρ Density
σ Surface Tension

INTRODUCTION

Heat transfer to impinging droplets on a surface is a complex problem. The highly transient nature of the process, combined with the short timescales and complex fluid mechanics involved in the expanding droplet make it a difficult problem to explore both analytically and experimentally. Despite this difficulty, however, many authors have explored the issue due to the topic's wide range of implications for spray cooling applications, ice formation (particularly on aircraft), and liquid metal deposits, among others.

Analytical work seeking to better understand and model this complex problem normally fall into one of two categories. The first, and more common approach, is to develop a numerical computer model, usually using a Volume-of-Fluid (VOF) approach, in order to model in entirety the velocity and temperature profiles in the impinging drop [1, 2]. This approach has the advantage of complete resolution of all relevant physics and is able to resolve the convection inside the droplet with high accuracy. This comes with the expense of high computational costs and run time, though, and resolving the fluid mechanics on a superhydrophobic (SH) surface would require too small of a spatial resolution.

*Address all correspondence to this author.

The second approach in modeling impinging heat transfer is to develop an analytical model for the heat transfer. The first proposed model by Pasandideh-Fard et al. outlined the estimated heat transfer just at point of maximum expansion and was included as a side note complementing a larger VOF model [3]. Later, Strotos et al. expanded on the framework and proposed an analytical solution by comparing their own VOF model to the one-dimensional analytical conduction solution for two contacting semi-infinite media [4]. The latest work has taken a similarity solution by Roisman et al. [5] and implemented it in the original framework to obtain a solution for the heat transfer over the expansion and retraction of the droplet [6].

Searle et al. developed an analytical model for the heat transfer to an impinging jet from SH surfaces [7]. Their model used the integral method which allowed inclusion of the temperature jump at the wall as a parameter in the model. Their work showed promise for a framework on resolving the heat transfer for SH surfaces.

No previous work has been done, however, which models the heat transfer to impinging drops on a SH surface for drops larger than micro-scale. This work outlines an analytical model which will approximate the heat transfer to an impinging drop on a SH surface.

BACKGROUND

When a water drop comes in contact with a surface it forms an angle that is determined by the surface energy of the material. The surface is denoted either hydrophilic ('wetting') or hydrophobic ('non-wetting') depending on if this angle is greater or less than 90° (see Figure 1). There are a few examples in nature, a lotus leaf for example, where a combination of surface chemistry and structure causes the surface to form a contact angle with the water larger than 150°. These surfaces, defined as a superhydrophobic (SH) surface, have numerous unique properties which are of interest for numerous engineering applications. The high droplet mobility present on the surface is beneficial for dropwise condensation applications as well as self-cleaning surfaces. For this reason attempts have been made to engineer SH surfaces in the lab and explore their properties and behavior.

To replicate this effect a micro or nano-scale structure is combined with a hydrophobic coating to achieve superhydrophobic effects. One approach is to use photolithography, the process used to create electronic chips, to etch a post or rib pattern in a silicon wafer. A thin film of Teflon is then applied to the wafer. This pattern allows the surface tension of the water to suspend the liquid above the micro-scale gaps present in the surface, greatly reducing the contact area of the drop. This pattern's effect is quantified by the cavity fraction, F_c. The cavity fraction is the percentage of the frontal area which is a cavity when viewed top-down on the surface. For some SH surfaces the cavity fraction can be as high as 0.93. This fraction, for a post surface (see

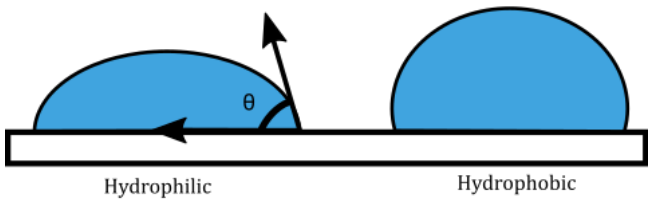

FIGURE 1. Demonstration of Different Boundary Conditions on SH surfaces.

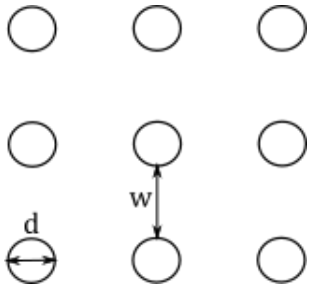

FIGURE 2. Diagram of typical post SH surface.

Figure 2) is

$$F_c = \frac{4w^2}{\pi d^2} \tag{1}$$

This reduction of contact area of the drop has unique effects on the hydrodynamics and heat transfer characteristics of the surface. Where the fluid is in contact with the surface the conventional no-slip boundary condition applies. Over the cavities, however, an approximately shear-free condition applies which allows a non-zero velocity at the surface. Since the percentage of a non-shear boundary condition is the majority for SH surfaces, an average slip-velocity boundary condition is applied to the surface on a macro level. This slip-velocity is expressed using the slip model proposed by Navier as

$$u_s = \lambda \left(\frac{\partial u}{\partial n} \right)_{wall} \tag{2}$$

where u_s is the aggregate slip velocity and λ is what's defined as the slip length [8]. Physically this length can be interpreted as the distance into the wall that the velocity profile would need to be

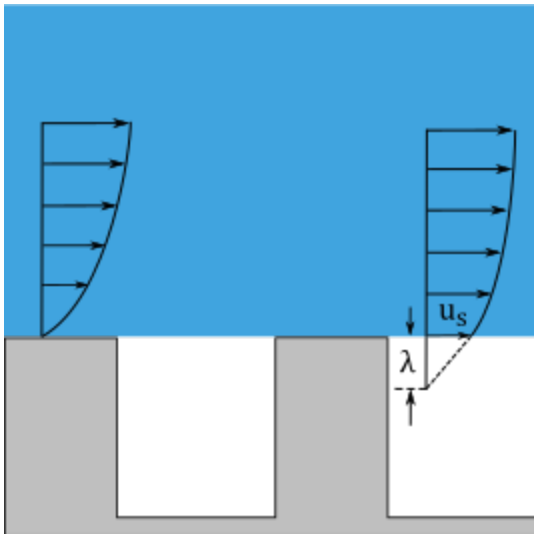

FIGURE 3. Demonstration of Different Boundary Conditions on SH surfaces.

extrapolated to reach the no-slip condition. This is a useful model as the slip length for a wide range of surface structure variants has been modeled. For a post surface, Ybert et al. outlined a model for the slip length as a function of the cavity fraction as

$$\frac{\lambda}{L} = \frac{0.325}{\sqrt{1-F_c}} - 0.44 \tag{3}$$

This average slip velocity has dramatic drag reduction effects and impacts the overall contact time of an impinging droplet on the surface. Similarly, for the heat transfer on a SH surface, the insulating regions of the air cavities greatly reduces the heat transfer expected on a SH surface and is expressed on a macro level as an average temperature jump at the wall, or

$$\Delta T_w = \lambda_T \left(\frac{\partial T}{\partial n}\right)_{wall} \tag{4}$$

METHODOLOGY

To model the heat transfer to the droplet both the hydrodynamics and the thermal transport have to be modeled. The hydrodynamic model developed by Clavijo et al. for droplet impingement on SH surfaces will be used and summarized here [9].

Hydrodynamic Model

A range of approaches have been used to model the hydrodynamics of impinging droplets. The most common was to develop a complete Volume-of-Fluid (VOF) computer model to resolve the entire velocity profile of the droplet [1,2]. For use in an analytical model, Pasandideh-Fard et al. used an expression for just the diameter at maximum expansion [3], while Strotos et al. used a normalized best-fit curve to their VOF data [4,6].

Attane et al. developed an analytical differential equation which balanced the kinetic energy, surface energy, and viscous dissipation of the drop to find the development of the radius of the drop over time [10]. They explored a number of various shapes and velocity profiles were explored before concluding the best approach was to model the droplet as a cylinder which flattens and expands over time.

Clavijo et al. expanded on this work by adding slip to the assumed velocity profile and energy equation [9]. Their results matched well with experiments conducted for a range of weber numbers and slip lengths. The velocity profile and resulting differential equation then become

$$\vec{V} = \begin{bmatrix} Cr(z+\lambda) \\ -C(z^2+2\lambda z) \end{bmatrix} \tag{5}$$

$$\begin{aligned} &\frac{d}{d\hat{t}}\left[\hat{R}^2(1-cos\Theta)+\frac{1}{3\hat{R}}\right] \\ &+\frac{1}{3888}\frac{d}{d\hat{t}}\left[\frac{1}{\hat{R}^{10}}\left(2\hat{\lambda}+\frac{1}{6\hat{R}^2}\right)^{-2}\left(\frac{d\hat{R}}{d\hat{t}}\right)^2\left(6\hat{R}^6\right.\right. \\ &\left.\left.+108\hat{\lambda}\hat{R}^8+648\hat{\lambda}^2\hat{R}^{10}+\frac{1}{5}+6\hat{\lambda}\hat{R}^2+48\hat{\lambda}^2\hat{R}^7\right)\right] \\ &+\frac{Oh}{3}\left(\hat{\lambda}+\frac{1}{12\hat{R}^2}\right)^{-2}\left(\frac{1}{18\hat{R}^6}+\frac{\hat{\lambda}}{\hat{R}^4}\right. \\ &\left.+\frac{6\hat{\lambda}^2}{\hat{R}^2}+\frac{1}{4}+\frac{s}{12\hat{R}^3}\right)\left(\frac{d\hat{R}}{d\hat{t}}\right)^2=0 \end{aligned} \tag{6}$$

where $s = 1.41Oh^{-2/3}$, $\hat{R} = R/D_0$, $\hat{\lambda} = \lambda/D_0$, and $\hat{t} = tV_0/\left(D_0\sqrt{We}\right)$. The radius expansion and retraction over time was compared to experiments with good results. Two boundary conditions are necessary to solve this problem. The first is found by ensuring that the initial surface energy of the cylindrical control volume is the same as the surface energy of the spherical droplet. The second is done by ensuring the kinetic energies of the two droplets are equal. This leads to

$$\frac{d\hat{R}_0}{d\hat{t}} = \frac{\left(2\hat{\lambda}+\hat{R}_0^2/6\right)\sqrt{324\hat{R}_0^{10}We}}{\sqrt{6\hat{R}_0^6+108\hat{\lambda}\hat{R}_0^8+648\hat{\lambda}^2\hat{R}_0^10+0.2+6\hat{\lambda}\hat{R}_0^2+48\hat{\lambda}^2\hat{R}_0^7}} \tag{7}$$

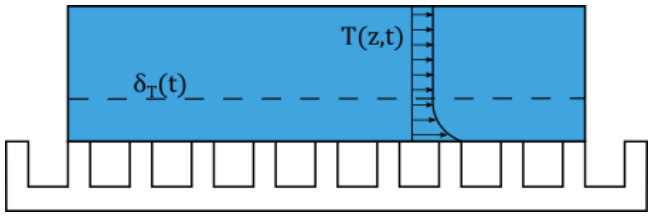

FIGURE 4. Control volume visualization for impingement model for SH surface using integral method. The energy is stored in the drop by allowing the boundary layer thickness, δ_T, to change with time.

Heat Transfer Model

The majority of previous analytical models for heat transfer to impinging drops use a parameter called the cooling effectiveness. Pasandideh-Fard et al. first proposed this parameter in 2000 [3] as a useful way to quickly summarize and normalize the heat transfer to a droplet as

$$\varepsilon(t) = \frac{\int_0^t \int_{A_c} q''(t)\, dA_c dt}{mc_p\,(T_c - T_{dr})} \tag{8}$$

For an analytical model, the instantaneous heat flux over time is needed. Searle et al. found an expression for the heat transfer on SH surfaces to jet impingement using the integral method with success [7]. The integral method involves assuming a temperature profile and integrating to the boundary layer and solving the energy equation on an integrated scale instead of the local scale. This method is a common approach to obtain heat transfer data without needing to resolve the exact temperature profile. Searle et al. also demonstrated the usefulness of the assumed temperature profile in allowing ready inclusion of the temperature slip length as a parameter, similar to the work by Clavijo et al. including slip length in the hydrodynamic model.

When applying the integral method to the case of impinging droplets an average boundary layer thickness is assumed. This is required because, unlike the case of jet impingement, the deformation of the droplet deforms the control volume which adds complexity to the energy balance. This method can be visualized in Figure 4. The boundary conditions of the temperature profile, then, are

$$T(z=0) = T_c - \Delta T_w \tag{9}$$

$$T(z=\delta_T) = T_{dr} \tag{10}$$

$$\frac{\partial T}{\partial t}(z=0) = 0 \tag{11}$$

where T_c is the contact temperature found for two contacting semi-infinite media by

$$T_c = \frac{\gamma_{liq} T_d + \gamma_{sol} T_w}{\gamma_{liq} + \gamma_{sol}} \tag{12}$$

The temperature profile then becomes

$$T(z,t) = T_c - \frac{2\lambda_T\,(T_c - T_{dr})}{2\lambda_T + \delta_T} - \frac{2\,(T_c - T_{dr})}{2\lambda_T + \delta_T} z + \frac{T_c - T_{dr}}{\delta_T\,(2\lambda_T + \delta_T)} z^2 \tag{13}$$

where applying Fourier's law allows the heat flux to be obtained, as

$$q_w'' = \frac{2k\,(T_c - T_d)}{2\lambda_T + \delta_T} \tag{14}$$

The heat flux at the wall, then, can be found once the boundary layer thickness over time is obtained. This is done by applying the energy equation to the droplet, assuming the same cylindrical shape that the hydrodynamic model uses. The energy equation for this case then is

$$q_w''(t)\,A = \frac{d}{dt}\left(\pi R^2 \int_0^H \rho c_p T\, dz\right) \tag{15}$$

The equation is solve by equating eqn 14 and eqn 15. The integral is found by breaking the integral as

$$\int_0^H T\, dz = \int_0^{\delta_T(t)} T\, dz + T_d(H(t) - \delta_T(t)) \tag{16}$$

The energy equation then, is

$$2\alpha \frac{T_c - T_d}{2\lambda_T + \delta_T} = \left(\frac{2\delta_T\,(T_c - T_d)}{3\,(2\lambda_T + \delta_T)} - \frac{\delta_T^2\,(T_c - T_d)}{3\,(2\lambda_T + \delta_T)^2}\right)\frac{\partial \delta_T}{\partial t} + \frac{\delta_T^2\,(T_c - T_d)}{R\,(2\lambda_T + \delta_T)}\frac{dR}{dt} \tag{17}$$

It should be noted that although there is no explicit convection term in the energy balance equation (due to the control volume encapsulating the entirety of the droplet) that convection effects are still captured with this model. The growth of the thermal boundary layer is influenced by two terms; the first is the conduction of heat through the contact area and the second is the expansion of the droplet which captures the convection induced by the expansion/flattening of the droplet over time. When the

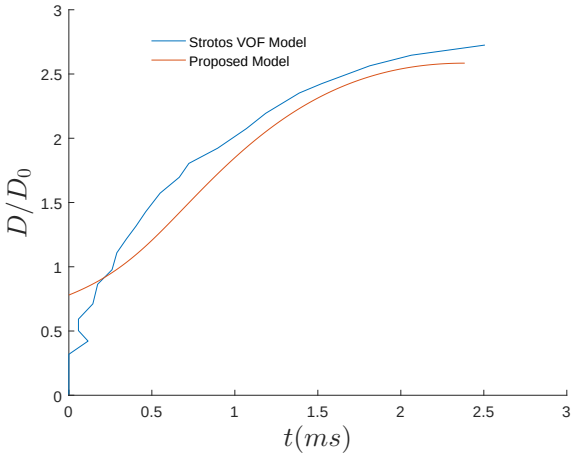

FIGURE 5. Diameter vs Time during expansion for Clavijo et al. model and Strotos VOF model for reference case.

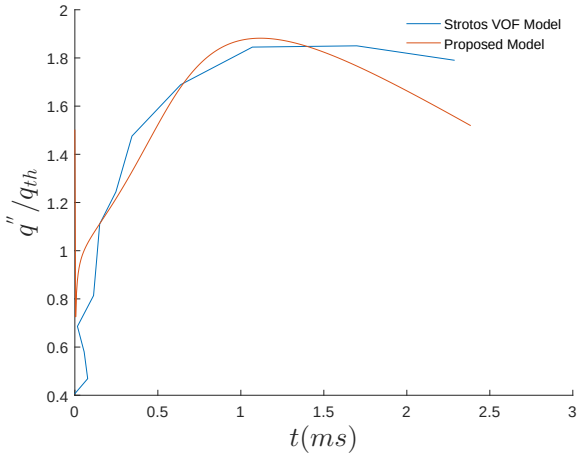

FIGURE 6. Heat Flux normalized by 1D Conduction Solution for Clavijo et al. model and Strotos VOF model for reference case.

droplet is expanding and cold water is moving towards the surface, $\frac{dR}{dt}$ is positive, and thus the growth of the thermal boundary thickness slows (or in extreme cases is negative) and the heat transfer at the wall is enhanced as expected.

RESULTS

The model was run first for the reference case listed by Strotos et al. and compared to their numerical VOF model to ensure the accuracy of the model on a standard, non-SH surface. The effect of slip length and contact angle was then explored for a range of Weber numbers.

Verification

Strotos et al. ran a VOF model for a reference case of an impinging droplet with a Weber number of 20 on a stainless steel surface at $60°C$. The VOF model had an advancing contact angle of $110°$, but a receding contact angle of only $10°$. Due to the capability of the Clavijo hydrodynamic model to only have a constant contact angle, only the heat transfer during the time up to maximum expansion of the droplet can be compared. The comparison between the hydrodynamic model can be seen in Figure 5.

In reporting their results, the instantaneous heat flux was normalized by the heat flux for one dimensional heat transfer between two contacting semi-infinite media. The exact solution to this problem, for reference, is

$$q''(t) = \frac{k_{liq}(T_c - T_w)}{\sqrt{\pi \alpha_{liq} t}} \tag{18}$$

The model comparison to the VOF model for the refence case can be seen in Figure 6. Due to the simplified assumption regarding an average boundary layer thickness, local differences are expected, but the overall trend closely matches that of the VOF model. As the droplet nears maximum expansion and the rate of expansion decreases, the effect of convection becomes minimal and the heat transfer enhancement begin to taper off. When this heat flux is integrated over the contact area over time to find the cooling effectiveness, these local differences average out and the model matches the VOF model, as seen in Figure 7. The end deviations in the predicted cooling effectiveness are within 25%. The under-prediction is largely due to the slight difference in predicted diameter of the droplet, which would effect the area integral in the cooling effectiveness calculation. Due to the demonstrated accuracy of the hydrodynamic model for SH surfaces this potential error source will be minimized.

Effect of Slip

For examining the effect of slip for various contact angles and Weber numbers, the model was run for a range of cases and the cooling effectiveness at the time of maximum expansion was plotted vs the normalized slip length. For all cases considered the thermal slip length was assumed to be equal to the velocity slip length.

The model was run for a wide range of contact angles for a Weber number of 50, as seen in Figure 8. It's apparent that the contact angle has little impact on the heat transfer expected. The Weber number, however, has a much larger impact on the heat transfer as can be seen in Figure 9.

In all cases, the heat transfer dramatically decreases as the surface becomes more and more superhydrophobic and the slip length increases.

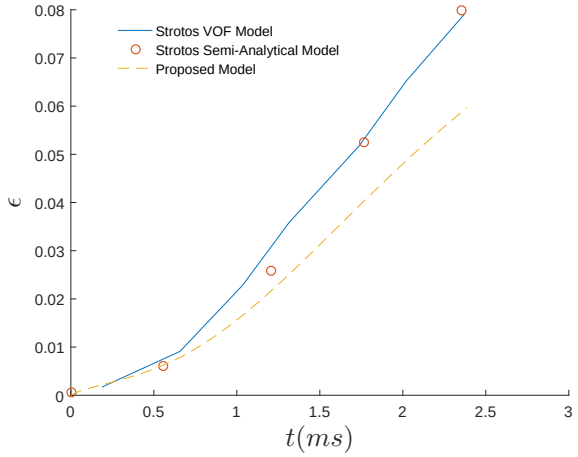

FIGURE 7. Cooling Effectiveness for Clavijo et al. model and Strotos VOF model for reference case.

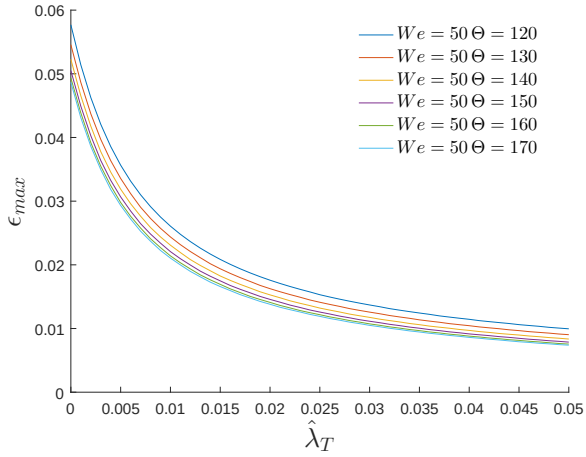

FIGURE 8. Cooling Effectiveness for Clavijo et al. model and Strotos VOF model for reference case.

CONCLUSIONS

The heat transfer to an impinging drop on a superhydrophobic surface was modeled. The hydrodynamics were modeled using a model outlined by Clavijo et al. with demonstrated accuracy in the range of Weber numbers considered [9]. The heat transfer model was developed using an integral method approach to obtain the cooling effectiveness of the drop over time. Verification of the model was completed by comparing to the reference case run in a numerical volume-of-fluid model developed by Strotos et al. [4]. The heat transfer was greatly reduced for superhydrophobic surfaces, with contact angle influencing the results little while the Weber number having a large impact on the results. This decreased amount of heat transfer to impinging drops

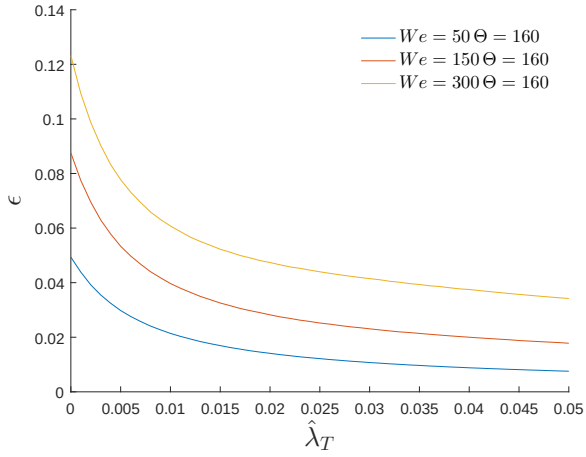

FIGURE 9. Cooling Effectiveness for Clavijo et al. model and Strotos VOF model for reference case.

on SH surfaces must be considered when selecting the potential use of SH surfaces.

ACKNOWLEDGMENT

This work was supported by the Utah NASA Space Grant Consortium.

REFERENCES

[1] PasandidehFard, M., Qiao, Y. M., Chandra, S., and Mostaghimi, J., 1996. "Capillary effects during droplet impact on a solid surface". *Physics of Fluids,* **8**(3), pp. 650–659.

[2] Strotos, G., Gavaises, M., Theodorakakos, A., and Bergeles, G., 2008. "Numerical investigation of the cooling effectiveness of a droplet impinging on a heated surface". *International Journal of Heat and Mass Transfer,* **51**(19), pp. 4728 – 4742.

[3] Pasandideh-Fard, M., Aziz, S., Chandra, S., and Mostaghimi, J., 2001. "Cooling effectiveness of a water drop impinging on a hot surface". *International Journal of Heat and Fluid Flow,* **22**(2), pp. 201 – 210.

[4] Strotos, G., Aleksis, G., Gavaises, M., Nikas, K.-S., Nikolopoulos, N., and Theodorakakos, A., 2011. "Non-dimensionalisation parameters for predicting the cooling effectiveness of droplets impinging on moderate temperature solid surfaces". *International Journal of Thermal Sciences,* **50**(5), pp. 698 – 711.

[5] ROISMAN, I. V., 2010. "Fast forced liquid film spreading on a substrate: flow, heat transfer and phase transition". *Journal of Fluid Mechanics,* **656**, p. 189204.

[6] Strotos, G., Nikolopoulos, N., Nikas, K.-S., and Moustris, K., 2013. "Cooling effectiveness of droplets at low weber numbers: Effect of temperature". *International Journal of Thermal Sciences,* **72**, pp. 60 – 72.

[7] Searle, M., Maynes, D., and Crockett, J., 2017. "Thermal transport due to liquid jet impingement on superhydrophobic surfaces with isotropic slip". *International Journal of Heat and Mass Transfer,* **110**, pp. 680 – 691.

[8] White, F. M., 2006. *Viscous Fluid Flow*, third ed. McGraw-Hill.

[9] Clavijo, C. E., Crockett, J., and Maynes, D., 2015. "Effects of isotropic and anisotropic slip on droplet impingement on a superhydrophobic surface". *Physics of Fluids,* **27**(12), p. 122104.

[10] Attan, P., Girard, F., and Morin, V., 2007. "An energy balance approach of the dynamics of drop impact on a solid surface". *Physics of Fluids,* **19**(1), p. 012101.